THE JOURNAL OF COMPARATIVE NEUROLOGY 509:594–607 (2008)

Postnatal Reorganization of Primary Afferent Terminal Fields in the Rat Gustatory Brainstem is Determined by Prenatal Dietary History

JAMIE E. MANGOLD[1] AND DAVID L. HILL[2]*
[1]Department of Psychiatry and Neurobehavioral Sciences, University of Virginia, Charlottesville, Virginia 22911
[2]Department of Psychology, University of Virginia, Charlottesville, Virginia 22904-4400

ABSTRACT

Dietary manipulation has been used as an experimental strategy to gain insight into the normal development of the gustatory system. Institution of a diet low in sodium chloride (NaCl) from embryonic day 3 (E3) to E12 (E3–E12 sodium-restricted rats) yields dramatically enlarged terminal fields of the chorda tympani (CT), greater superficial petrosal (GSP), and glossopharyngeal (IX) nerves in the rostral pole of the nucleus of the solitary tract (NTS) at adulthood. To examine how this early, limited dietary manipulation affects postnatal terminal field development, we used a triple anterograde nerve label procedure at postnatal day 15 (P15), P25, P35, and ≥P40 (adults) in two groups: rats fed a commercial diet replete in sodium (controls) and E3–E12 sodium-restricted rats. Results showed an age-related decrease in terminal field volumes of all three nerves during normal development. In contrast, E3–E12 sodium-restricted rats displayed age-related increases of the CT and IX terminal fields, with the terminal field volume of the GSP remaining unchanged throughout development. NTS volume did not grow after P15; therefore, alterations in terminal field volumes are not due to parallel alterations in the size of the NTS. Our data suggest that the age-related decrease in terminal fields observed in controls may reflect activity-dependent pruning of afferent terminals, whereas terminal field increases seen in E3–E12 sodium-restricted rats may reflect cellular/molecular differences in the NTS induced predominantly by activity-independent mechanisms. These findings predict a significant difference in the development of neural coding and sensory-guided behaviors between E3–E12 sodium-restricted rats and controls. J. Comp. Neurol. 509:594–607, 2008.

Indexing terms: chorda tympani; greater superficial petrosal; glossopharyngeal; brainstem nuclei; gustatory nerves; taste; salt; diet; nucleus of the solitary tract

Environmental manipulation has been used as an experimental tool for understanding the normal development of sensory systems, including the taste system (Lasiter, 1991, 1995; Pittman and Contreras, 2002). The experimental strategy of manipulating early dietary exposure has provided many insights into both peripheral (Hill and Przekop, 1988; Krimm and Hill, 1999; Shuler et al., 2004) and central (Lasiter, 1995; Lasiter and Kachele, 1990) gustatory development. For example, the introduction of a low-sodium diet (0.03% NaCl) during the early embryonic development that is continued throughout adulthood has profound effects on afferent nerve terminal field organization in the rostral portion of the nucleus of the solitary tract (NTS; King and Hill, 1991; Krimm and Hill, 1997; May and Hill, 2006). When a low-sodium diet is introduced for a limited, early prenatal period, even greater changes are induced in terminal fields in the NTS (Krimm and Hill, 1997; Mangold and Hill, 2007). That is,

Grant sponsor: National Institutes of Health; Grant number: DC00407.

*Correspondence to: Dr. David L. Hill, Department of Psychology, P.O. Box 400400, University of Virginia, Charlottesville, VA 22904.
E-mail: dh2t@virginia.edu

Received 6 August 2007; Revised 27 January 2008; Accepted 25 April 2008

DOI 10.1002/cne.21760

Published online in Wiley InterScience (www.interscience.wiley.com).

paradoxically, a low-sodium diet fed to pregnant rats only from embryonic day 3 (E3) to E12 results in larger terminal fields of the chorda tympani (CT), greater superficial petrosal (GSP), and lingual branch of the glossopharyngeal (IX) nerves than terminal fields of lifelong sodium-restricted rats and in rats "recovered" from sodium restriction late in postnatal development but before adulthood (Mangold and Hill, 2007). As an important aside, projections of the IX to brainstem areas other than the NTS (i.e., spinal trigeminal nucleus) are unaffected by the dietary restriction from E3 to E12 (Mangold and Hill, 2007), suggesting that the rearrangement of terminal fields in the brainstem is selective.

The enlarged terminal fields in E3–E12 sodium-restricted rats are especially surprising because the rats received a sodium-replete diet before the taste system was established (Mistretta, 1972). The widespread alterations in E3–E12 sodium-restricted rats are not due to increased numbers of ganglion cells, increased target size, or obvious changes in peripheral taste function; these measures are similar to controls (Mangold and Hill, 2007). Moreover, gross alterations in taste bud numbers and innervation of peripheral targets in rats with a lifelong period of dietary sodium restriction do not occur (Krimm and Hill, 1999). Therefore, it is unclear how the abnormal morphology seen at adulthood is established.

Examination of terminal field development in E3–E12 sodium-restricted rats may help in understanding the underlying cellular/molecular mechanism(s) involved in the establishment of drastically altered terminal field organization at adulthood. For example, we recently discovered that the CT terminal field in controls decreases in size as neural activity increases, leading to the hypothesis of activity-dependent "pruning" of exuberant processes over the course of postnatal development (Sollars et al., 2006). Findings from experiments with rats experiencing lifelong dietary sodium restriction are consistent with this hypothesis: CT nerve function is frozen at an immature stage (Hill, 1987) that predictably results in a lack of terminal field "pruning" (Sollars et al., 2006).

The current study not only aims to characterize the morphological developmental process(es) leading to grossly enlarged terminal fields in adult E3–E12 sodium-restricted rats but also characterizes the normal anatomical postnatal development of terminal fields in control rats. The morphology of the CT, GSP, and IX terminal fields and the overlaps among terminal fields were examined in both E3–E12 sodium-restricted rats and control rats at P15, P25, P35, and ≥P40 (adults). Our data show that all three afferent nerve terminal fields in the gustatory NTS undergo an age-related decrease in volume over normal development. In contrast, 9 days of maternal sodium restriction results in a different developmental trend: an extended postnatal increase in terminal field volume. This indicates that profound changes evident at adulthood resulting from a gestational dietary manipulation have their origins in abnormal postnatal development that is programmed prenatally.

MATERIALS AND METHODS

NTS Terminal Field Volumes

Animals. All experiments were endorsed by the Animal Care and Use Committee at the University of Virginia and followed guidelines set by the National Institutes of Health. Rats were purchased from Harlan Sprague-Dawley. Forty-six Sprague-Dawley rats aged P15–P16 (n = 11), P25 (n = 10), P35 (n = 11), ≥P40 (n = 14; adults) were used for afferent nerve labeling (see below).

Dietary conditions. Control animals (n = 23) received a standard, commercial diet of 0.3% NaCl rat chow (Harlan Teklad Rodent Diet 8604; Harlan Teklad, Madison, WI) and tap water ad libitum. E3–E12 sodium-restricted rats (n = 23) received low-sodium rat chow (0.03% NaCl; MP Biomedicals, Solon, OH) and distilled water ad libitum via their mothers from E3 to E12 as described previously (Mangold and Hill, 2007).

To determine the date of conception, female rats were checked for sperm every morning during breeding. When females were sperm positive, they were moved to a separate cage and placed on a low-sodium diet 3 days later (E3). Nine days after being placed on the low-sodium diet (E12), the mothers were placed on a normal diet for the remainder of gestation, and the pups were maintained on a normal diet from birth until the time of the taste nerve labeling procedure (P15–P16, P25, P35, ≥P40). The date of birth was defined as P0.

Triple-fluorescent anterograde taste nerve labeling. Procedures used to label three nerves with fluorescent tracers were similar to those described by May and Hill (2006) and Mangold and Hill (2007). Specifically, the CT, GSP, and IX nerves were labeled with anterograde tracers to determine the volume and spatial organization among the afferent nerve terminal fields in the rostral NTS during postnatal development. The density of the label was not quantified because of inaccuracies inherent in making and interpreting density measurements at the light microscopic level. Therefore, the terminal field volumes were calculated when any label, regardless of density, was present. This provides data on the topographical organization of the terminal fields but does not provide information concerning the absolute amount of afferent input into the NTS.

Rats were sedated with a 0.32 mg/kg injection of Domitor (medetomidine hydrochloride: Pfizer Animal Health, Exton, PA; I.M.) and anesthetized with 40 mg/kg Ketaset (ketamine hydrochloride: Fort Dodge Animal Health, Fort Dodge, IA; I.M.). A water-circulating heating pad was used to maintain body temperature. All rats except for those aged P15–P16 were positioned in a nontraumatic head holder. A ventral approach was taken in all rats to expose the CT and GSP nerves within the right tympanic bulla. The CT and GSP nerves were cut near the geniculate ganglion in the tympanic bulla and dimethyl sulfoxide (DMSO; Fisher Scientific Company, Fair Lawn, NJ) was briefly applied to the cut nerves. Crystals of 3-kD biotinylated dextran amine were then applied to the proximal cut end of the GSP and 3 kD Texas red dextran amine was applied to the proximal cut end of the CT (Fig. 1). A mixture of Vaseline and mineral oil was applied to prevent migration of dye. The IXth nerve was isolated just medial to the tympanic bulla and was cut and placed on a small piece of parafilm. Again, DMSO was applied briefly (~60 seconds) and crystals of 3-kD Cascade blue dextran amine were applied to the proximal cut end of the nerve (Fig. 1). All dextran amine conjugates were purchased from Invitrogen (Carlsbad, CA). The Vaseline and mineral oil mixture and a layer of parafilm were placed on top of the IXth nerve to keep the dye in place. Animals were then

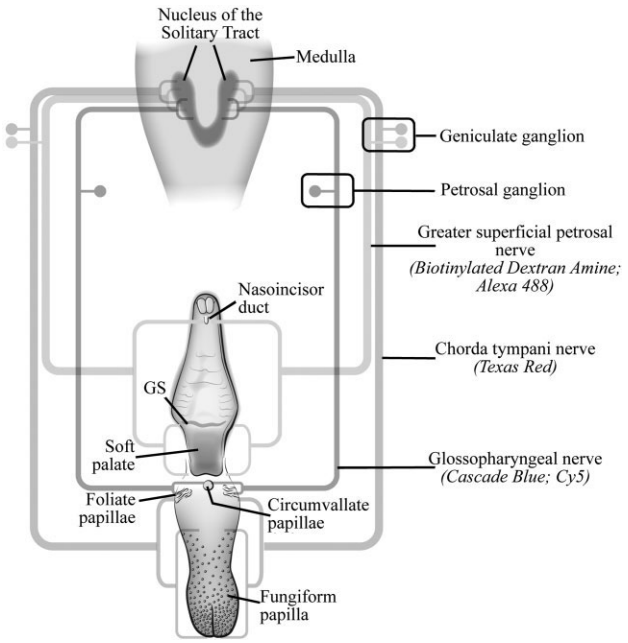

Fig. 1. Anatomical organization of the peripheral gustatory system and the first central synaptic relay in the nucleus of the solitary tract (NTS). The chorda tympani nerve innervates taste buds in fungiform and foliate papillae on the anterior tongue. The greater superficial petrosal nerve innervates taste buds in the nasoincisor duct, the geschmacksstreifen (GS), and the soft palate. Both nerves make up the VIIth cranial nerve (facial nerve) and have cell bodies in the geniculate ganglia. The glossopharyngeal nerve innervates taste buds in foliate and circumvallate papillae on the posterior tongue and has cell bodies in the petrosal ganglia. All three nerves terminate in the ipsilateral NTS. The fluorescent markers used to detect each terminal field are noted in parentheses. See Materials and Methods for a detailed description.

injected with 5 mg/kg Antisedan (atipamezole hydrochloride: Pfizer Animal Health; I.M.) to promote reversal of anesthesia. After an 18–24-hour survival, animals were deeply anesthetized with 4 mg/kg urethane (ethyl carbamate: Sigma-Aldrich Co., St. Louis, MO; I.P.) and transcardially perfused with Krebs-Henseleit buffer (pH 7.3), followed by 8% paraformaldehyde in PBS (pH 7.2).

We established previously (May and Hill, 2006) that 1) tracers placed on a nerve did not inadvertently label other nerves, 2) the full complement of fibers were labeled as revealed by examinations of the respective ganglia, and 3) the period of survival postsurgery was optimal for transport of each anterograde tracer. It should be noted that the mere presence of labeled terminal fields from GSP, CT, or IX axons does not necessarily mean that they convey taste information. For example, the three nerves also supply temperature and tactile information (Frank, 1968; Ogawa et al., 1968; Smith et al., 1988; Sollars and Hill, 1998). Thus, the NTS is a highly integrative center for multiple sensory inputs.

Tissue preparation. After perfusions, brains were removed and postfixed in 8% paraformaldehyde overnight. The medulla was blocked and sectioned horizontally on a vibratome at 50 μm to allow visualization of the entire rostral-caudal and medial-lateral extent of the afferent nerve terminal fields in the NTS. Tissue sections were collected in 0.1 M phosphate-buffered saline (PBS; pH 7.2) at room temperature. Sections were then incubated for 1 hour in PBS containing 0.2% Triton with 1:500 streptavidin Alexa Fluor 488 (Invitrogen) and 1:500 rabbit anti-Cascade blue (Invitrogen) at room temperature. Streptavidin Alexa Fluor 488 was used to visualize the biotinylated dextran amine-labeled GSP-positive terminals (Figs. 1, 2). The rabbit anti-Cascade blue was used as a primary antibody directed at Cascade blue-labeled IX nerve-positive terminals (Fig. 1). Next, sections were rinsed in PBS (3 × 5 minutes) and then incubated for 30 minutes in PBS containing 0.2% Triton and 1:500 goat anti-rabbit Cy5 (Jackson Immunoresearch, West Grove, PA). Goat anti-rabbit Cy5 was used as a secondary antibody to visualize IX nerve terminals (Figs. 1, 2). Finally, sections were rinsed in PBS and imaged on a confocal scanning laser microscope (Fluoview 300; Olympus America, Melville, NY).

Confocal microscopy and data collection for horizontal sections. Terminal fields were imaged with an Olympus IX70 microscope fitted with a Fluoview 3.3 laser scanning system (Olympus America, Melville, NY) and equipped with a 488-nm argon laser, a 543-nm green He/Ne laser, and a 633-nm red He/Ne laser. Each 50-μm section containing fluorescent label was wet mounted between two coverslips, and optical sections of each terminal field were captured sequentially every 3 μm. Images of all three terminal fields were digitally merged, and terminal field areas and areas of overlap among terminal fields were quantified in Neurolucida software (version 4.34; MicroBrightField, Colchester, VT; Fig. 2). The volume of terminal fields and the fields of overlap in each 50-μm section were calculated by summing the areas in each optical section and multiplying by the optical section thickness (3 μm). Total terminal field volume and overlaps were obtained by summing the volumes from each 50-μm section.

For figure plates, Volocity (Improvision, Inc., Lexington, MA) and Illustrator and Photoshop (Adobe Systems, San Jose, CA) were used to compose images from digital files in which all optical sections for each physical section were flattened into one plane. Images were enhanced only for contrast and brightness.

Statistical analysis. The mean ± SEM was determined for total nerve terminal field volume, total overlap among terminal fields, and volumes of terminals contained within dorsal, intermediate, and ventral zones (see Results for definition of zones). These variables were compared across ages (within dietary groups) and within ages (between dietary groups) of control and E3–E12 sodium-restricted rats by using an ANOVA and LSD post hoc tests. Statistical results from post hoc analysis are reported with the corresponding P value. An α level of $P \leq 0.05$ was considered as statistically significant.

Coronal section confocal microscopy. To illustrate further the overlapping terminal fields in relation to NTS subnuclei, we labeled the three nerves as described earlier in a P15 E3–E12 sodium-restricted rat and then viewed the fields in coronally sectioned tissue. Because terminal field volumes of P15 control and P15 E3–E12 sodium-restricted rats were generally similar, as indicated by analysis of horizontal sections, we chose to present only a representative coronal section from a P15 E3–E12 sodium-restricted rat. Coronal sections from adult control and adult E3–E12 sodium-restricted rats were described previously (Mangold and Hill, 2007). One optical section

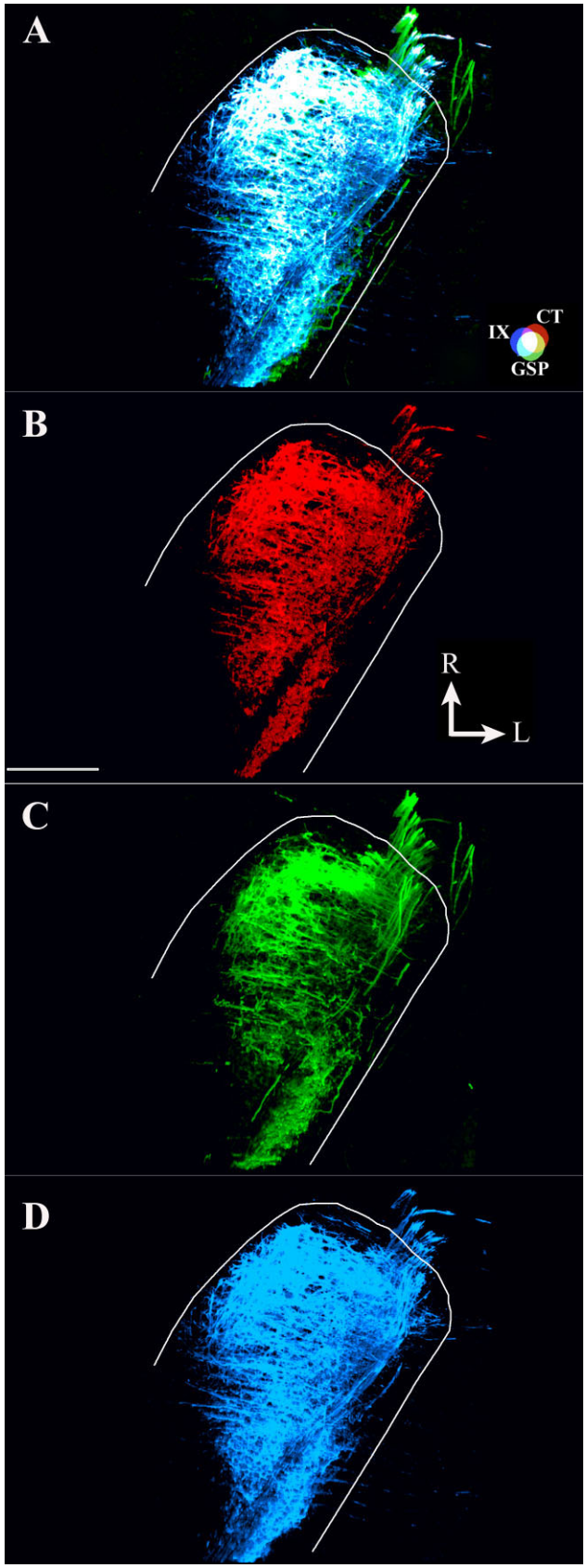

using transmitted light was also imaged to show the respective terminal fields overlayed with the approximate location of NTS subnuclei. Finally, each section was mounted on a slide and subsequently stained with cresyl violet to show the NTS and other dorsal medullary structures. No measurements were taken from coronal sections; they were used to examine terminal field organization in the coronal plane only.

Total NTS volume

Animals. Thirty-one Sprague-Dawley rats were used for total NTS volume measurements [control: P15–P16, n = 4; P25, n = 4; P35, n = 4; ≥P40 (adult), n = 3; E3–E12: P15–P16, n = 4; P25, n = 4; P35, n = 5; ≥P40 (adult), n = 3]. The majority of these animals were also used for the triple nerve labeling and terminal field data collection. Rats were deeply anesthetized with 4 mg/kg urethane (ethyl carbamate: Sigma-Aldrich Co.; I.P.) and transcardially perfused at P15–P16, P25, P35, and ≥P40 with Krebs-Henseleit buffer (pH 7.3) followed by 8% paraformaldehyde (pH 7.2).

Tissue preparation and confocal microscope transmitted light imaging. The procedure has been described previously (Mangold and Hill, 2007). Briefly, brains were removed and postfixed in 8% paraformaldehyde overnight. The medulla was blocked and sectioned in the horizontal plane on a vibratome at 50 μm and collected and prepared for imaging as described above. Sections were imaged on the scanning confocal microscope using the transmitted light function with the 488-nm argon laser. The NTS is relatively translucent within the brainstem and appears similar to phase-contrast images when imaged with the transmitted light.

Data collection. The NTS volume was measured in Neurolucida computer software (version 4.34; MicroBrightField). To calculate volume, the measurements from all the sections were summed and multiplied by the section thickness (50 μm).

Statistical analysis. Mean total NTS volumes were compared among ages within each group and between control and E3–E12 sodium-restricted adults and analyzed by using an ANOVA and LSD post hoc tests. Statistical results with an α level of $P \leq 0.05$ were reported as significant.

RESULTS

Total terminal field volume

Controls. Control rats displayed a general trend in which all three terminal fields (IX, GSP, and CT) were largest at P15 and decreased in size throughout development (Figs. 3 A–H, 4, solid lines and symbols). There were

Fig. 2. Components of fluorescent images from a P15 control rat. Fluorescent photomicrographs show the three merged terminal fields (**A**) and the component images of the CT (red; **B**), GSP (green; **C**), and IX (blue; **D**) terminal fields. The approximate location of the NTS is outlined in white. The CT-GSP overlap is shown as yellow, IX-GSP overlap is shown as blue-green, IX-CT overlap is shown as magenta, and the CT-GSP-IX terminal field overlap is shown as white. Refer to color guide in A. Rostral (R) and lateral (L) are indicated in B. Scale bar = 200 μm.

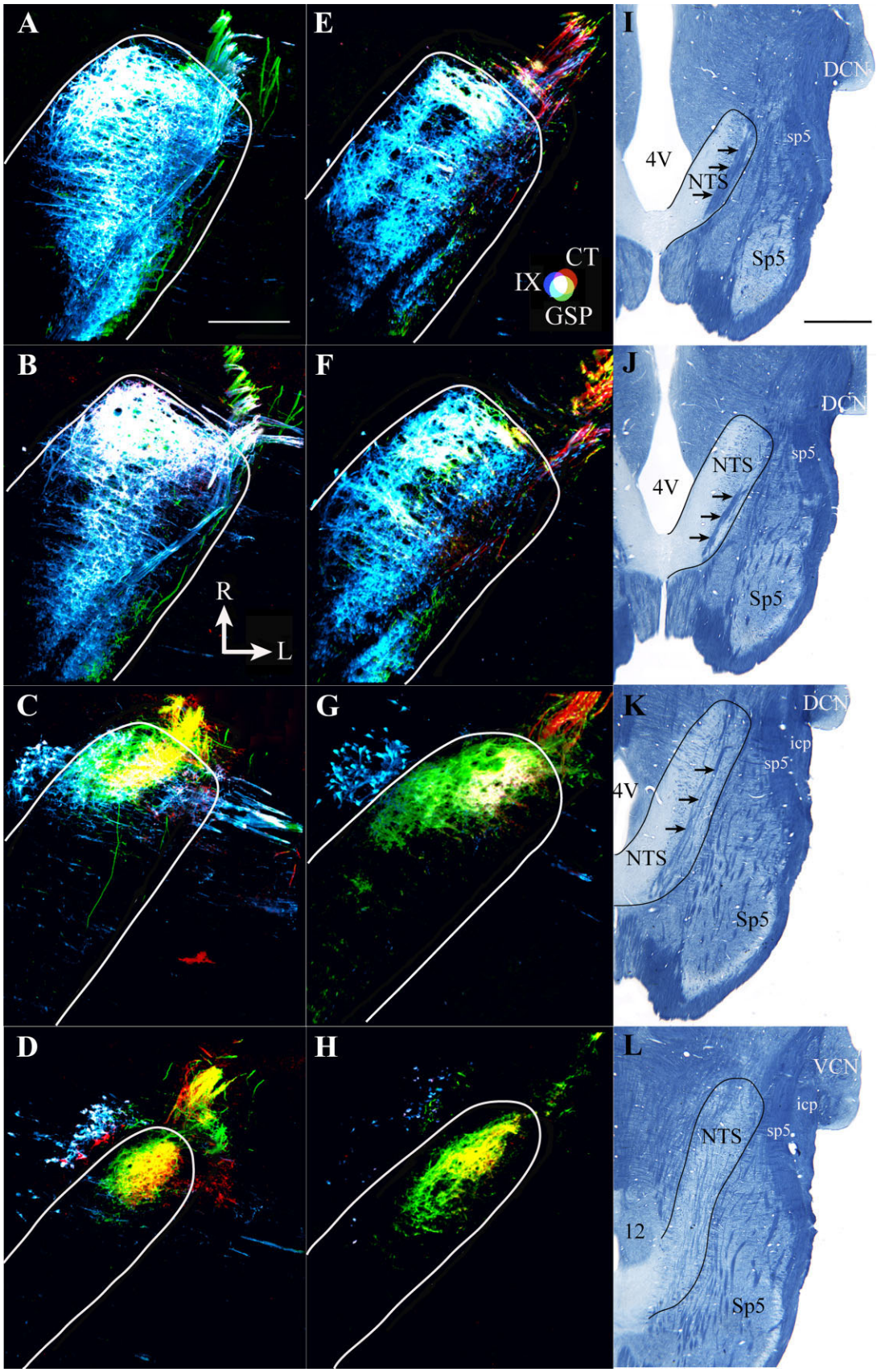
A
E
I
DCN
sp5
4V
NTS
Sp5
CT
IX
GSP
B
F
J
DCN
NTS
sp5
4V
Sp5
R
L
C
G
K
DCN
icp
sp5
4V
NTS
Sp5
D
H
L
VCN
icp
NTS
sp5
12
Sp5

Figure 3

differences, however, in the age at which the terminal fields matured.

At P15, the total terminal field volumes for the IX, CT, and GSP were the largest of all ages examined in controls (Figs. 3A–D, 4). Figure 3A–D shows the terminal fields in horizontal section from a control rat aged P15. Each of the three terminal fields is large, and clear regions of overlap exist among all three terminal fields in the dorsal sections (Fig. 3A,B). It is also apparent that the GSP and CT terminal fields have extensive zones of overlap (Fig. 2), even into the ventral sections (Fig. 3C,D). In contrast, Figure 3E–H shows that the terminal fields in adult control rats are generally smaller and have fewer zones of overlap. As seen in Figure 4, each of the total terminal field volumes in controls decreased by approximately half during the 10 days between P15 and P25 (Fig. 4A, IX, $P = 0.0001$; Fig. 4B, CT, $P = 0.0001$; Fig. 4C, GSP, $P = 0.0001$). It was at P25 when IX and GSP terminal field volumes reached maturity. IX and GSP terminal field volumes at P35 did not significantly differ from terminal field volumes at adulthood (Fig. 4A,C; $P = 0.30$ and $P = 0.10$, respectively). This, however, was not the developmental pattern for the CT terminal field, in that it also decreased significantly in volume between P25 and P35 (Fig. 4B; $P = 0.005$); the total terminal volume for the CT did not decrease in volume thereafter (Fig. 4B). Therefore, at P35, the terminal fields of all three nerves achieved mature shape and size (Figs. 3E–H, 4).

E3–E12 sodium-restricted rats. In stark contrast to the pattern of normal development, E3–E12 sodium-restricted rats displayed an increase in total terminal field volume with increasing age. IX, CT, and GSP total terminal field volumes were large at P15 (Fig. 4, dashed lines and open symbols; Fig. 5A–D), and all remained relatively stable until P35 (IX: P15–P25, $P = 0.75$; P25–P35, $P = 0.93$; CT: P15–P25, $P = 0.21$; P25–P35, $P = 0.91$; GSP: P15–P25, $P = 0.75$; P25–P35, $P = 0.64$). Surprisingly, both IX (Fig. 4A; $P = 0.0001$) and CT terminal fields (Fig. 4B; $P = 0.0001$) more than doubled in size between P35 and adulthood, whereas GSP terminal fields did not change significantly (Figs. 4C, 5E–H; $P = 0.62$).

Fig. 3. Horizontal sections of merged images from dorsal through ventral gustatory NTS in control rats. Fluorescent photomicrographs of P15 control rat (**A–D**) and a ≥P40 (**E–H**) rat (adult). The approximate location of the NTS is outlined in white. The most dorsal sections (A and E) are characterized by the presence of substantial amounts of terminal field overlap, but with more overlapping field evident in P15 control rats (A). Dorsal sections in B and F contain all three terminal fields, with more overlap occurring in P15 rats (B). Intermediate sections (C and G) are characterized by the densely labeled oval shape of the CT terminal field and retrogradely labeled cells of the salivatory nucleus, outside and medial to the NTS. Note that in P15 rats IX terminal field is present (C), where it normally does not project in adult controls (G). Ventral sections contain CT and GSP terminal fields and retrogradely labeled cells of the salivatory nucleus (D and H). Nerve terminal field and overlap colors are the same as noted in Figure 2 and are shown on the color guide in E. Myelin-stained brainstem sections from an adult rat fed the control diet are shown in **I–L** to illustrate brainstem landmarks characteristic of the dorsal to ventral zones. The NTS is outlined in black, and arrows point to the solitary tract. Rostral (R) and lateral (L) are indicated (B). 4V, fourth ventricle; 12, hypoglossal nucleus; DCN, dorsal cochlear nucleus; icp, inferior cerebellar peduncle; NTS, nucleus of the solitary tract; Sp5, spinal trigeminal nucleus; sp5, spinal trigeminal tract; VCN, ventral cochlear nucleus. Scale bars = 200 μm in A (applies to A–H); 1 mm in I (applies to I–L).

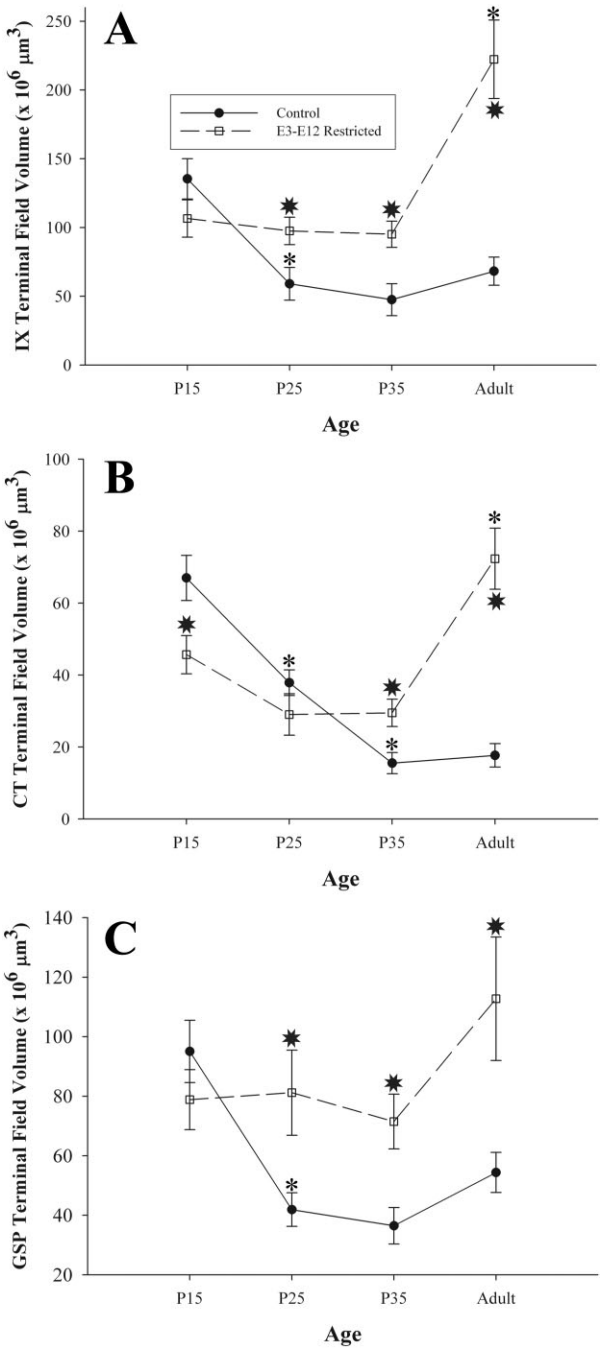

Fig. 4. Mean total terminal field volumes (±SEM) across developmental ages in control (solid lines and symbols) and E3–E12 sodium-restricted rats (dashed lines and open symbols) for IX (**A**), CT (**B**), and GSP (**C**). The small asterisks denote a significant difference ($P < 0.05$) from the preceding age for that nerve terminal field, and the large asterisks denote a significant difference ($P < 0.05$) from the respective control group.

Group-related comparisons. As a result of different patterns of terminal field development between controls and E3–E12 sodium-restricted rats, there were group-related differences during postnatal development for each nerve. At P15, the IX terminal field volumes were similar

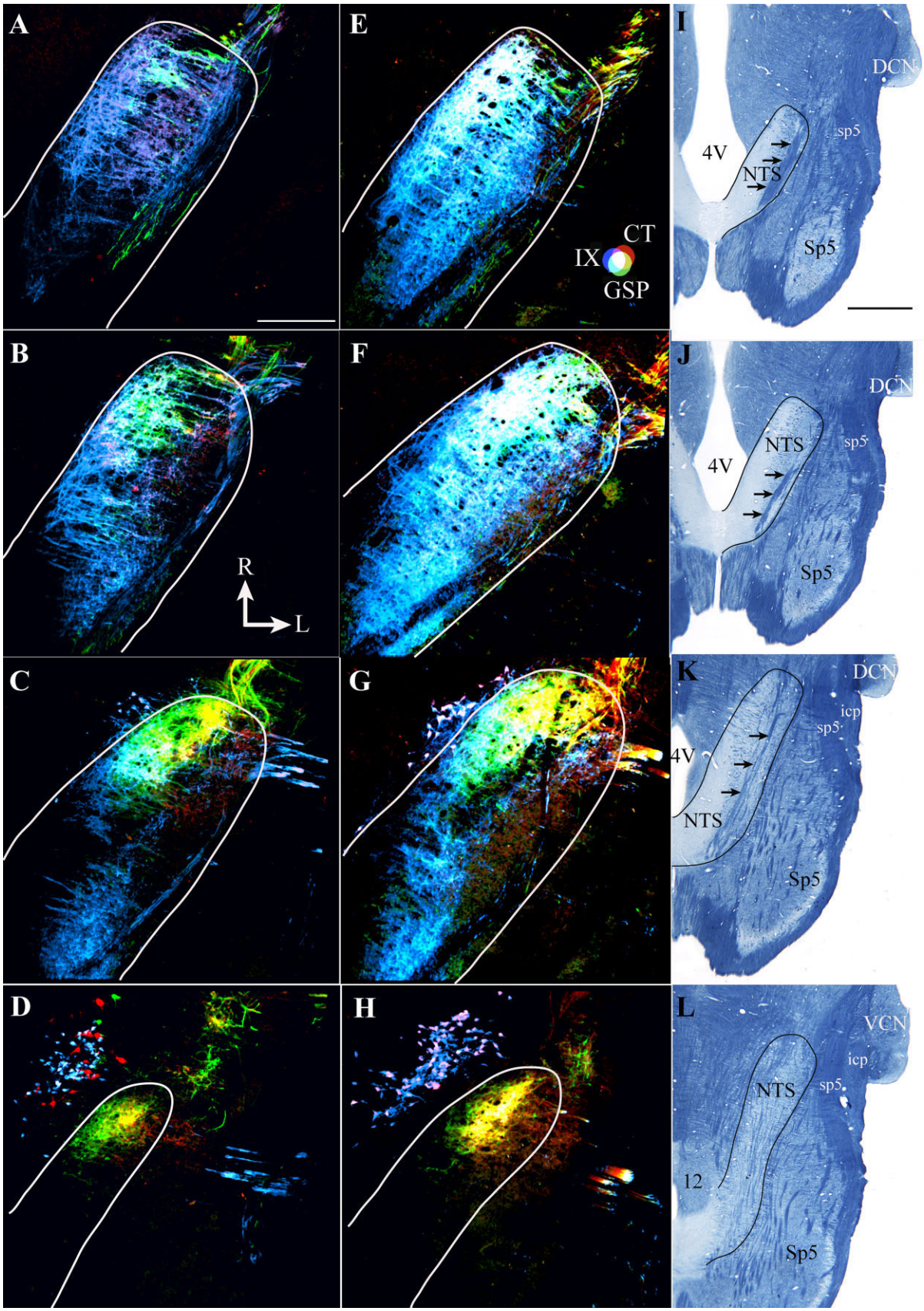
A
E
I
DCN
sp5
4V
NTS
Sp5
CT
IX
GSP
B
F
J
DCN
NTS
sp5
4V
Sp5
R
L
C
G
K
DCN
icp
sp5
4V
NTS
Sp5
D
H
L
VCN
icp
NTS
sp5
12
Sp5

Figure 5

between controls and E3–E12 sodium-restricted rats (Fig. 4A). However, at P25, IX terminal field volumes began to deviate between groups in that the volumes in E3–E12 sodium-restricted rats were significantly greater than in controls (Fig. 4A; $P = 0.04$). The IX terminal field volume in E3–E12 rats remained larger than that in controls at P35 ($P = 0.04$), with the difference further increasing to almost fourfold at adulthood (Fig. 4A; $P = 0.0001$). The GSP displayed the same trend, in that the terminal fields in E3–E12 sodium-restricted rats were significantly larger at P25 ($P = 0.03$), P35 ($P = 0.04$), and adulthood compared with controls (Fig. 4C; $P = 0.0001$). The CT terminal field volume, however, was different between groups at P15, P35, and adulthood (Fig. 4B). Specifically, the terminal field of the CT nerve was larger in controls at P15 ($P = 0.01$); groups were similar at P25 ($P = 0.26$) and larger in E3–E12 restricted rats at P35 ($P = 0.02$) and approximately five times larger in adults ($P = 0.0001$).

Overlap among terminal fields follow total terminal field development

The overlap among terminal fields also decreased with increasing age in controls and increased with age in E3–E12 sodium-restricted rats. It appears qualitatively (compare Figs. 3 with 5) and quantitatively (Fig. 6) as though the organization of the terminal fields in E3–E12 sodium-restricted rats "grows" to match the organization seen in P15 control rats. Control rats begin with the terminal fields relatively indistinct from each other through extensive overlapping terminal fields and then mature into the three terminal fields with distinct characteristics. Conversely, E3–E12 rats begin with somewhat distinct features and then develop relatively indistinct features.

Between P15 and P25, all volumes of overlapping terminal fields in controls decreased in size: IX with GSP (Fig. 6A; $P = 0.0001$); CT with GSP (Fig. 6B; $P = 0.0001$); IX with CT (Fig. 6C; $P = 0.001$); and IX, CT, and GSP (Fig. 6D; $P = 0.001$). By comparison, only terminal fields that overlapped with the CT terminal field decreased in size between P25 and P35 days in controls: CT with GSP (Fig. 6B; $P = 0.01$); IX with CT (Fig. 6C; $P = 0.03$); and IX, CT, and GSP (Fig. 6D; $P = 0.05$). At P35, terminal field volumes did not differ from adult terminal field volumes (Fig. 4); therefore, overlaps among terminal fields also did not differ between P35 and adulthood (Fig. 6A–D).

In E3–E12 sodium-restricted rats, there were no changes in terminal field overlap among nerves from P15 to P25 (Fig. 6; IX-GSP overlap, $P = 0.77$; CT-GSP overlap, $P = 0.21$; IX-CT overlap, $P = 0.10$; IX-CT-GSP overlap, $P = 0.28$) and from P25 to P35 (Fig. 6; IX-GSP overlap, $P = 0.65$; CT-GSP overlap, $P = 0.91$; IX-CT overlap, $P = 0.96$; IX-CT-GSP overlap, $P = 0.84$). Therefore, the volumes of terminal field overlap from the three nerves were constant throughout this period. However, the amount of terminal field overlap approximately doubled between P35 and adulthood for CT with GSP (Fig. 6B; $P = 0.0001$); IX with CT (Fig. 6C; $P = 0.001$); and IX, CT, and GSP (Fig. 6D; $P = 0.002$). This was due to the increase in the overall total IX and CT terminal field volume between these ages (Fig. 4).

Comparisons between the two dietary groups revealed that the terminal fields generally began with similar overlapping terminal field volumes early in postnatal development and then diverged with age (Fig. 6). The exception was that the CT with GSP terminal field overlap in P15 sodium-restricted rats was 31% smaller than in controls (Fig. 6B; $P = 0.04$). After P15, the overlapping terminal field volumes diverged throughout development between dietary groups, similar to that noted for the total terminal field volumes of each nerve (Figs. 3–5). Specifically, the IX with GSP terminal field overlaps in P25, P35, and adult sodium-restricted rats were at least two times larger than in age-matched controls (Fig. 6A; P25, $P = 0.006$; P35, $P = 0.002$; adult, $P = 0.015$). The CT with GSP, IX with CT, and IX with CT with GSP overlapping terminal field volumes in P35 and adult rats were also significantly greater than in controls (Fig. 6B–D; Ps ≤ 0.03). For example, the volume of the overlapping field between the IX and CT was over twelve times larger in E3–E12 sodium-restricted rats compared with controls (Figs. 3E–H, 5E–H, 6C). The volumes of the CT with GSP, IX with CT, and IX with CT overlapping terminal fields were not significantly different in P25 rats (Fig. 6).

Zonal distribution of terminal fields. To analyze further the terminal fields in developing control rats, we divided the NTS into dorsal, intermediate, and ventral zones as described previously (Mangold and Hill, 2007; May and Hill, 2006). Briefly, the dorsal zone contained sections in which the solitary tract was most visible, the fourth ventricle occupied the largest medial-lateral extent, and the spinal trigeminal tract extended rostrally to approximately the same level as the rostralmost extent of the NTS (Fig. 3I,J). This was the largest of the three zones, encompassing almost the entire IX terminal field in controls (Fig. 3A,B,E,F). The intermediate zone was characterized by the decrease in the fourth ventricle volume compared with the dorsal zone, by the dorsal extent of the hypoglossal nucleus, by the extension of the spinal trigeminal tract rostrally beyond the inferior cerebellar pedun-

Fig. 5. Horizontal sections of merged images from dorsal through ventral gustatory NTS in E3–E12 sodium-restricted rats. Fluorescent photomicrographs are shown for a P15 E3–E12 restricted (**A–D**) and adult E3–E12 (**E–H**) restricted rat. The approximate location of the NTS is outlined in white. The most dorsal sections in P15 E3–E12 restricted rats (A) are characterized by the presence of the IX terminal field and a slight GSP terminal field; however, in adult E3–E12 restricted rats, CT terminal field can also be seen (E). Dorsal sections in B and F contain all three terminal fields, with more overlap occurring in adult rats (F). Intermediate sections (C and G) are characterized by the densely labeled oval shape of the CT terminal field and retrogradely labeled cells of the salivatory nucleus, outside and medial to the NTS. Note that, in adult rats (G), more IX terminal field is present than is seen in P15 rats (C). Also note that these images are from individual rats; therefore, the size of the specific fields shown does not necessarily correspond exactly with the group mean (e.g., the terminal field for the IX shown in G is larger than the mean for the group). Ventral sections contain CT and GSP terminal fields and retrogradely labeled cells of the salivatory nucleus (D and H). Note that there is more CT-GSP overlap in H compared with D because of a larger CT terminal field. Nerve terminal field and overlap colors are the same as noted in Figure 2 and are shown on the color guide in E. Myelin-stained brainstem sections from an adult rat fed the control diet are shown in **I–L** to illustrate brainstem landmarks characteristic of the dorsal to ventral zones. The location of the landmarks and size of the NTS did not differ qualitatively between groups or with age. The NTS is outlined in black, and arrows point to the solitary tract. Rostral (R) and lateral (L) are indicated (B). 4V, fourth ventricle; 12, hypoglossal nucleus; DCN, dorsal cochlear nucleus; icp, inferior cerebellar peduncle; NTS, nucleus of the solitary tract; Sp5, spinal trigeminal nucleus; sp5, spinal trigeminal tract; VCN, ventral cochlear nucleus. Scale bars = 200 μm in A (applies to A–H); 1 mm in I (applies to I–L).

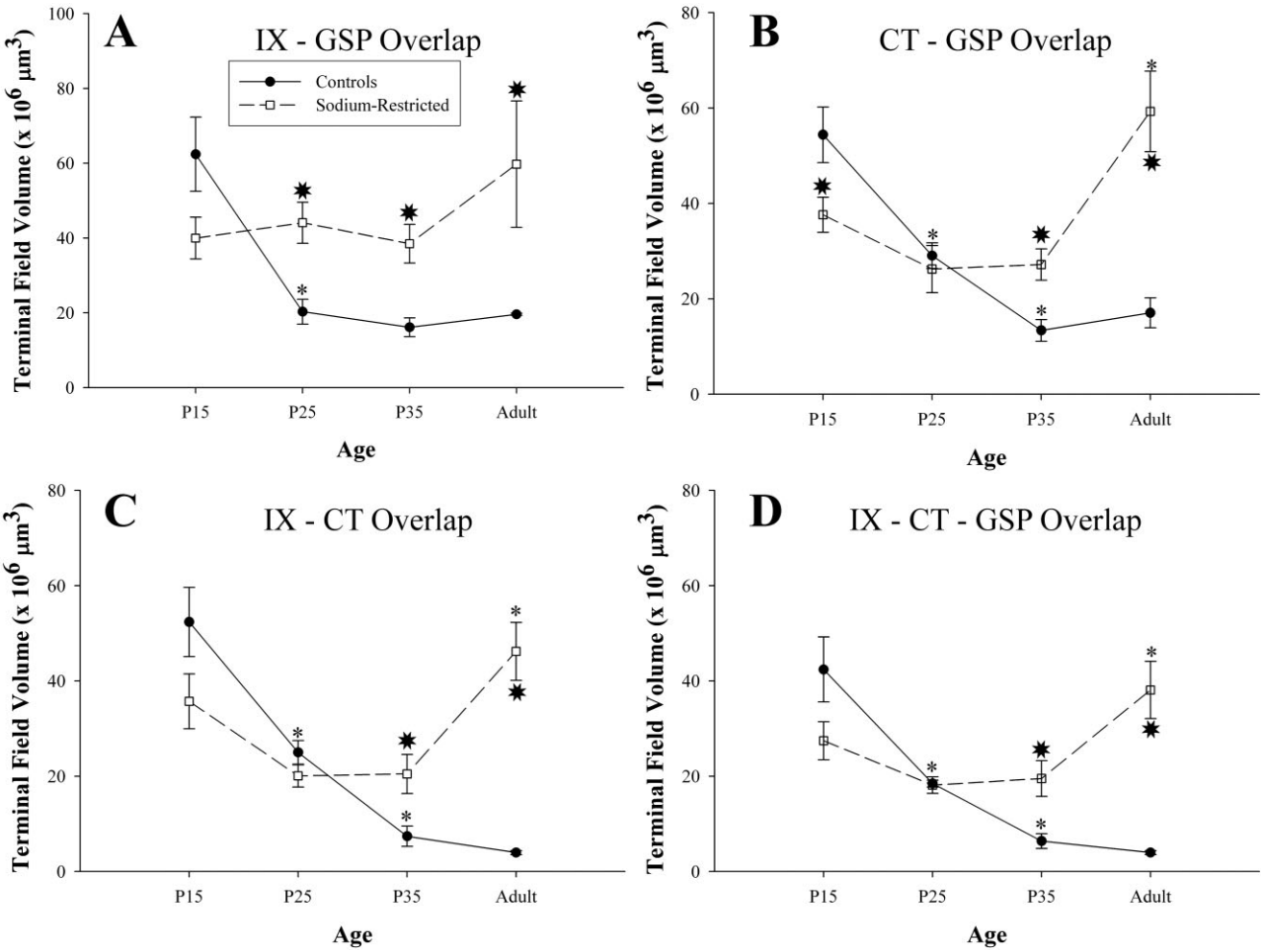

Fig. 6. Mean total volumes (±SEM) of overlapping terminal fields across developmental ages in control (solid lines and symbols) and E3–E12 sodium-restricted rats (dashed lines and open symbols) for IX with GSP overlap (**A**), CT with GSP overlap (**B**), IX with CT overlap (**C**), and IX with CT with GSP overlap (**D**). The small asterisks denote a significant difference ($P < 0.05$) from the preceding age for that nerve terminal field, and the large asterisks denote a significant difference ($P < 0.05$) from the respective control group.

cle, and by the presence of the dorsal extent of the facial nucleus (Fig. 3K). The ventral zone of the terminal fields had an expanded hypoglossal nucleus and facial nucleus compared with the intermediate sections (Fig. 3L). We note that the orientation of the NTS within the brainstem is such that the caudalmost portion of the NTS is dorsal to the rostralmost portion (see Mangold and Hill, 2007). That is, the NTS extends ventrally and rostrally from the dorsal most extent of the NTS. Therefore, the "dorsal" zone more accurately represents the dorsal-caudal portion of the field in the NTS, and the intermediate and ventral sections represent a more ventral-rostral portion of the terminal field in the NTS.

As found previously in adult controls (Mangold and Hill, 2007; May and Hill, 2006), the dorsal to ventral appearance and expansion of the three terminal fields in the NTS were similar throughout development. Specifically, IX terminations entered the NTS most dorsally, followed by GSP terminations and then CT terminations. In the dorsal zone of controls, IX ($P = 0.002$), CT ($P = 0.003$), and GSP ($P = 0.002$) terminal field volumes decreased between P15 and P25 (Table 1). Similarly, all terminal field volume overlaps in the dorsal zone in controls decreased significantly from P15 to P25: IX with GSP ($P = 0.001$); CT with GSP ($P = 0.003$); IX with CT ($P = 0.003$); and IX, CT, and GSP ($P = 0.002$; Table 1). There was a further decrease in terminal field overlaps that contained the CT terminal field between P25 and P35 in the dorsal zone (CT with GSP, $P = 0.03$; IX with CT, $P = 0.02$; IX, CT, and GSP, $P = 0.04$; Table 1). Changes were also evident in the intermediate zone of the NTS for the CT and IX terminal fields. Volumes decreased between P15 and P25 for the IX ($P = 0.04$) and CT ($P = 0.01$) terminal fields (Table 1). Consequently, the overlap among all terminal fields in controls that included CT terminal field in the intermediate zone decreased between P15 and P25 (IX with GSP, $P = 0.04$; CT with GSP, $P = 0.004$; IX with CT, $P = 0.008$; IX, CT, and GSP, $P = 0.01$; Table 1). Terminal field volumes in the ventral zone did not differ (Table 1).

Similar to that described for controls, the terminal fields in the NTS in E3–E12 sodium-restricted rats were analyzed by dorsal to ventral zones (Fig. 5I–L). There were no differences in IX or CT terminal field volumes in the dorsal zone in E3–E12 sodium-restricted rats from P15 to

TABLE 1. Mean (SEM) Terminal Field Volumes ($\times 10^6$ μm^3) by Dorsal to Ventral Zones

DORSAL

	TOTAL VOLUMES			OVERLAPPING VOLUMES			
	IX	CT	GSP	IX & GSP	CT & GSP	IX & CT	IX & CT & GSP
Control							
P15 (n=6)	127.9 (13.8)	51.1 (6.7)	67.0 (10.1)	56.5 (9.5)	39.5 (6.3)	48.3 (7.1)	38.1 (6.5)
P25 (n=4)	*66.3 (7.1)	*29.0 (3.0)	*32.1 (3.8)	*22.5 (2.5)	*21.1 (1.6)	*24.4 (2.4)	*17.9 (0.9)
P35 (n=5)	43.9 (10.2)	*9.6 (3.2)	22.2 (5.3)	14.0 (2.4)	*7.7 (2.6)	*6.3 (2.3)	*5.3 (1.7)
Adult (n=7)	67.7 (10.4)	8.8 (2.0)	32.3 (4.5)	19.2 (0.3)	8.4 (1.9)	3.9 (0.5)	3.9 (0.5)
E3 – E12 Restricted							
P15 (n=5)	102.2 (12.0)	32.2 (4.9)	52.7 (8.1)	36.4 (5.6)	28.4 (3.2)	33.2 (5.2)	25.0 (3.9)
P25 (n=5)	92.0 (10.8)	23.4 (5.8)	57.7 (12.5)	39.3 (5.6)	20.7 (4.9)	17.9 (3.2)	16.0 (2.6)
P35 (n=6)	90.5 (12.1)❋	18.1 (4.3)	46.1 (6.6)	33.9 (5.8)❋	16.6 (3.7)	16.3 (4.4)	15.1 (3.8)❋
Adult (n=7)	*217.3 (27.7)❋	*52.0 (7.0)❋	77.7 (17.0)❋	*62.3 (12.7)❋	*41.7 (6.7)❋	*43.5 (5.5)❋	*35.5 (5.3)❋

INTERMEDIATE

	TOTAL VOLUMES			OVERLAPPING VOLUMES			
	IX	CT	GSP	IX & GSP	CT & GSP	IX & CT	IX & CT & GSP
Control							
P15	7.3 (2.6)	13.1 (1.9)	19.1 (4.6)	5.1 (2.0)	12.9 (1.5)	5.6 (1.8)	3.8 (1.3)
P25	*0.8 (0.8)	*7.4 (1.4)	10.1 (2.7)	*0.4 (0.4)	*7.0 (1.5)	*0.4 (0.4)	*0.6 (0.4)
P35	4.1 (2.6)	5.2 (0.5)	11.0 (3.1)	2.1 (1.6)	5.0 (0.5)	1.0 (0.6)	1.1 (0.6)
Adult	0.5 (0.5)	6.5 (1.0)	15.2 (1.7)	0.4 (0.4)	6.4 (1.0)	0.1 (0.1)	0.1 (0.1)
E3 – E12 Restricted							
P15	4.4 (2.3)	12.7 (0.6)	21.9 (1.9)	3.5 (1.7)	12.2 (0.7)	2.5 (1.1)	2.5 (1.1)
P25	4.7 (3.4)	*4.8 (0.9)	16.7 (5.1)	3.9 (3.0)	*4.7 (0.9)	1.6 (1.1)	1.6 (1.1)
P35	5.1 (1.5)	7.7 (1.0)	18.2 (4.2)	3.7 (1.3)	6.2 (1.7)	2.5 (0.6)	2.5 (0.6)
Adult	5.0 (2.3)	*16.9 (2.6)❋	29.1 (5.4)❋	4.5 (2.7)	*15.6 (2.8)❋	3.3 (2.0)	3.2 (2.0)

VENTRAL

	TOTAL VOLUMES			OVERLAPPING VOLUMES			
	IX	CT	GSP	IX & GSP	CT & GSP	IX & CT	IX & CT & GSP
Control							
P15	0 (0)	2.5 (1.0)	7.3 (1.4)	0 (0)	2.6 (1.2)	0 (0)	0 (0)
P25	0 (0)	1.4 (0.6)	2.3 (0.7)	0 (0)	1.3 (0.5)	0 (0)	0 (0)
P35	0 (0)	0.7 (0.2)	3.3 (0.9)	0 (0)	0.7 (0.2)	0 (0)	0 (0)
Adult	0 (0)	2.1 (0.7)	6.3 (1.4)	0 (0)	2.0 (0.6)	0 (0)	0 (0)
E3 – E12 Restricted							
P15	0 (0)	0.7 (0.3)	3.4 (1.8)	0 (0)	0.6 (0.3)	0 (0)	0 (0)
P25	0 (0)	0.3 (0.1)	4.1 (1.6)	0 (0)	0.3 (0.1)	0 (0)	0 (0)
P35	0 (0)	1.1 (0.5)	5.5 (2.4)	0 (0)	*1.0 (0.5)	0 (0)	0 (0)
Adult	0 (0)	4.5 (1.4)	7.4 (1.1)	0 (0)	*3.0 (0.8)	0 (0)	0 (0)

* Significantly different ($p<0.05$) from the preceding age group.
❋ Significantly different ($p<0.05$) from corresponding control group.

P35 (Table 1). However, between P35 and adulthood, IX ($P = 0.0001$) and CT ($P = 0.0001$) terminal field volumes more than doubled (Table 1). Similarly, the amounts in which terminal fields overlapped doubled in the dorsal zone between P35 and adulthood were IX with GSP overlap ($P = 0.04$); CT with GSP overlap ($P = 0.01$); IX with CT overlap ($P = 0.001$); and IX, CT, and GSP overlap ($P = 0.002$; Table 1). The GSP terminal field volume remained stable throughout development in the dorsal zone (i.e., P15 to adulthood; Table 1). In the intermediate zone, there was a decrease in CT terminal field between P15 and P25 ($P = 0.006$) and a later increase in CT terminal field between P35 and adulthood ($P = 0.0001$; Table 1). Between P15 and P25, the CT with GSP terminal field overlap decreased slightly ($P = 0.02$) and then increased slightly again in the intermediate zone between P35 and adulthood ($P = 0.001$; Table 1). In the ventral zone, there was an increase in the CT with GSP terminal field overlap between P25 and P35 and again between P35 and adulthood (Ps = 0.008; Table 1).

The group-related differences in the dorsal zone mirrored the differences seen in the total terminal field volumes (Figs. 4, 6, Table 1). Namely, the means of all terminal fields in the dorsal zone were greater in E3–E12 sodium-restricted rats at adulthood than in controls (IX, $P = 0.0001$; CT, $P = 0.0001$; GSP, $P = 0.001$; IX with GSP, $P = 0.0001$; CT with GSP, $P = 0.0001$; IX with CT, $P = 0.0001$; IX with CT with GSP, $P = 0.0001$; Table 1). The terminal fields in the dorsal zone of E3–E12 sodium-restricted rats aged P35 were also larger than in age-matched controls for the IX terminal field ($P = 0.03$) and the overlapping terminal fields of IX with GSP ($P = 0.04$) and IX with CT with GSP ($P = 0.05$; Table 1). Finally, the terminal field volumes of the CT ($P = 0.0001$), GSP ($P = 0.01$), and CT with GSP overlap ($P = 0.0001$) in the intermediate zone in adult E3–E12 sodium restricted rats were larger than those in adult controls (Table 1). No group-related differences were found in the ventral zone.

The relatively widespread effect in the dorsal zone (across ages and between dietary groups) may be a function of the relatively large portion of the total terminal field occupied by the dorsal compared with intermediate and ventral zones. That is, there simply may be more area

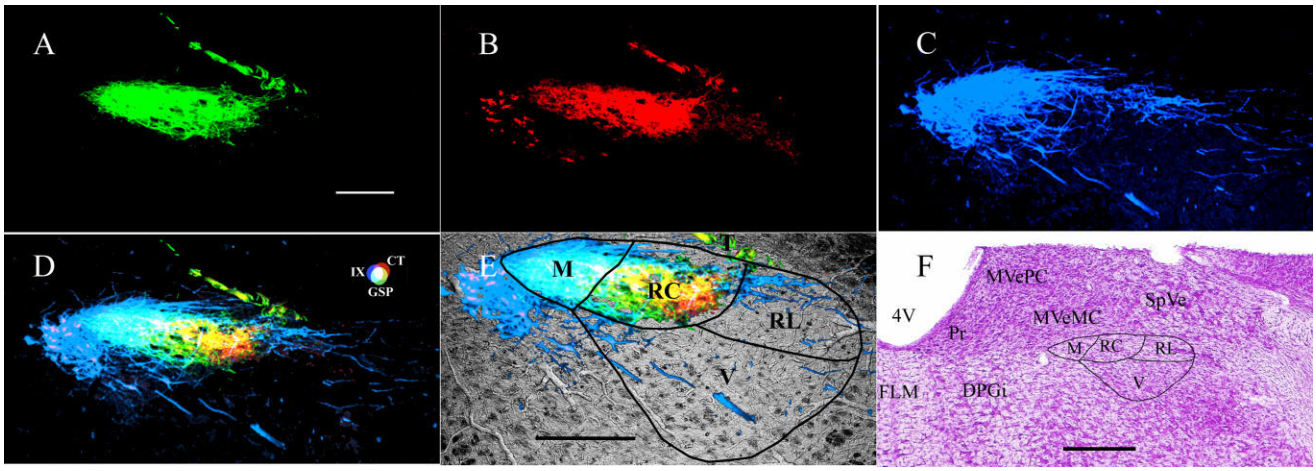

Fig. 7. Terminal fields within subdivisions of the NTS in a P15 E3–E12 sodium-restricted rat. Coronal section through the rat medulla in a P15 E3–E12 sodium-restricted rat showing the terminal field for the GSP (**A**), CT (**B**), and IX (**C**) nerves. **D** shows the merged terminal fields. **E** shows the merged image superimposed on an image of the brainstem obtained through the transmitted light channel on the confocal laser microscope system. **F** shows Nissl-stained tissue illustrating the location of the NTS relative to other brainstem structures. Lines in E and F demarcate the approximate boundaries of the subdivisions in the NTS as described by Halsell et al. (1996) and Whitehead (1990). Note that, although terminal fields are large, they seem to be contained within appropriate subnuclei. Refer to the color guide in D to identify individual fields and overlap among different terminal fields. D, dorsal; L, lateral; T, solitary tract; M, medial subdivision of the NTS; RC, rostral central subdivision of the NTS; V, ventral subdivision of the NTS; RL, rostral lateral subdivision of the NTS; 4V, fourth ventricle; DPGi, dorsal paragigantocellular nucleus; FLM, fasciculus longitudinalis medialis; MVeMC, medial vestibular nucleus magnocellular; MVePC, medial vestibular nucleus parvocellular; Pr, principal nucleus; SpVe, spinal vestibular nucleus. Scale bars = 200 μm in A (applies to A–E); 400 μm in F.

in which alterations can occur without connoting functional or cytoarchitectonically defined subdivisions.

Description of enlarged terminal fields as they relate to NTS subnuclei: coronal sections

The photomicrographs presented in Figure 7 are from a P15 E3–E12 sodium-restricted rat and were taken approximately 400 μm caudal to the anteriormost extent of the NTS (see also Figs. 3, 5). Thus, sections used here were from the caudal extent of the "rostral" pole, which also contains the "intermediate" zone of the NTS (Mangold and Hill, 2007). This area was chosen to correspond to adult control and adult E3–E12 sodium-restricted coronal sections previously described by us (Mangold and Hill, 2007). The distinct overlap of the three fields can be readily seen in Figure 7D. This figure illustrates that the enlarged terminal fields of P15 E3–E12 sodium-restricted rats did not occupy inappropriate NTS subnuclei (Fig. 7E). Specifically, the CT and GSP projected almost exclusively to the rostral-central subnucleus and the IX projected to the same subnucleus, but also extended medially to the medial subnucleus (Fig. 7E). These data are consistent with the labels shown in horizontal sections (e.g., Fig. 5B), where the IX terminal field extended to the medial border of the NTS and the CT and GSP terminal fields were located relatively more lateral and overlapping with that of the IX. It should be noted that the borders of the subnuclei shown in Figure 7E and duplicated for Figure 7F were drawn from the transmitted image shown in Figure 7E before the terminal field photomicrograph was overlaid on the transmitted image. Although our determination of subnuclei borders used unstained tissue, unlike the stained tissue used by others (Halsell et al., 1996; Whitehead, 1990), the boundaries for the subdivisions of NTS subnuclei shown in Figure 7E,F are similar to those shown by Halsell et al. (1996). Retrogradely labeled cells of the salivatory nucleus are also evident (Fig. 7B–D).

NTS volume

We demonstrated previously that NTS size did not differ between adult control and E3–E12 sodium-restricted rats (Mangold and Hill, 1997). The current results showed that NTS volume also did not differ as a function of age or group over the course of postnatal development (control: P15, 11.0×10^8 μm^3 ± 0.9; adult, 9.8×10^8 μm^3 ± 0.04, $P = 0.44$; E3–E12 sodium-restricted: P15, 10.5×10^8 μm^3 ± 0.8; adult, 9.5×10^8 μm^3 ± 0.03, $P = 0.34$). Therefore, NTS sizes in all groups and ages were similar.

DISCUSSION

These contrasting results show dramatically different programs of terminal field development of nerves that carry gustatory information resulting from different prenatal dietary histories. Control rats exhibit a relatively early postnatal period of terminal field rearrangements that are characterized by decreases in terminal field volumes, whereas E3–E12 sodium-restricted rats exhibit stable terminal fields until relatively late in preadult development, at which age there is an increase in terminal field volumes.

In E3–E12 sodium-restricted rats, all three terminal fields are visible at P15, volumes of all terminal fields remain constant until P35, and then the CT and IX terminal fields become significantly larger at adulthood, at which age there is an impressive amount of overlap among terminal fields (Fig. 8A). In contrast to E3–E12 sodium-

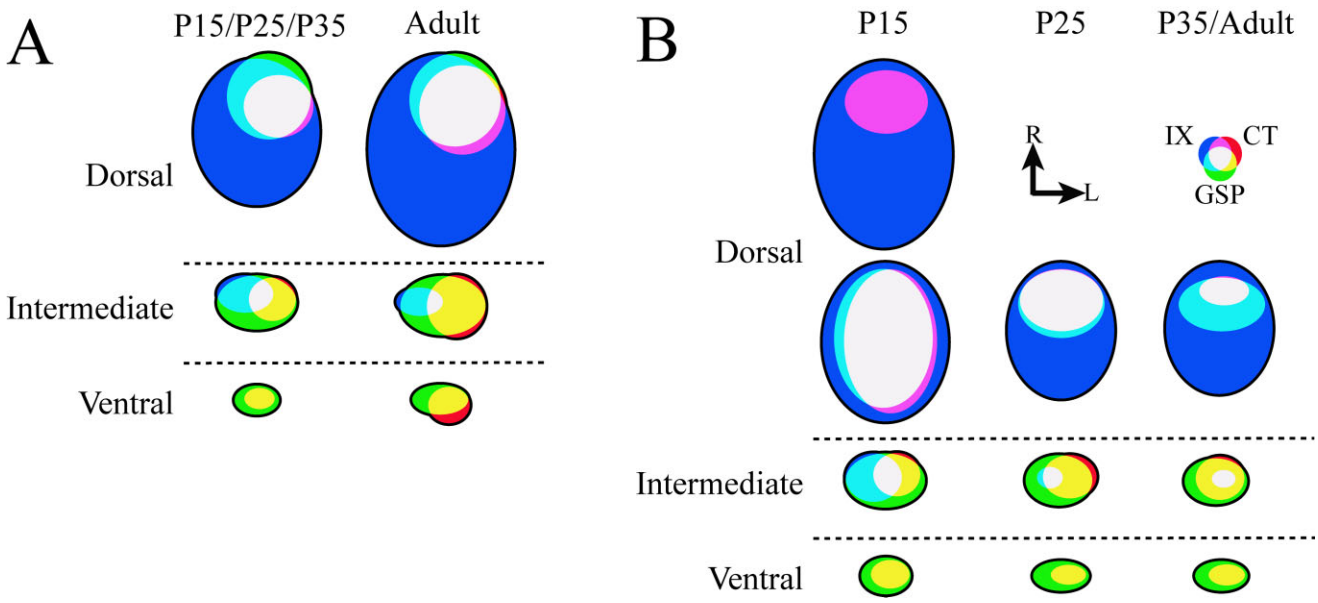

Fig. 8. **A:** Summary model of terminal field development in E3–E12 sodium-restricted rats. Model of terminal field organization through the dorsal-ventral extent of horizontal sections from the right NTS in P15/P25/P35 E3–E12 sodium-restricted (left column) and adult E3–E12 sodium-restricted rats (right column). Overlapping fields are represented at the dorsal, intermediate, and ventral fields. Note that CT and IX terminal fields are larger at adulthood. See Results for details of the overlap among the three fields and a comparison of age-related differences. **B:** Summary model of terminal field development in control rats. Model of terminal field organization through the dorsal-ventral extent of horizontal sections from the right NTS in P15 control (left column), P25 control (middle column), and P35/adult control rats (right column). Overlapping fields are represented at the dorsal, intermediate, and ventral fields. A dorsal section is shown containing terminal fields in P15 control rats that are not present in the other two groups. See Results for details of the overlap among the three fields and a comparison of age-related differences. Refer to orientation guide for rostral (R) and lateral (L) directions, and the color guide to identify individual fields among different terminal fields. The overlap colors are the same as noted in Figure 2. Note: Because of the orientation of the NTS within the brainstem, the term "dorsal" section refers to dorsal-caudal, and "ventral" refers to ventral-rostral.

restricted rats, control rats display a trend of decreasing terminal field size for all three nerves; however, maturation of specific terminal fields occurs at different ages (Fig. 8B). All three terminal fields are large at P15 and decrease in size by approximately 50% at P25. It is at P25 when both the GSP and the IX nerve terminal fields reach their mature morphology. The CT terminal field undergoes another significant decrease in volume between P25 and P35; no significant changes occur thereafter. Thus, the terminal fields of these three nerves reach mature shape and size by P35 (Fig. 8B).

Comparison with previous developmental studies

Our findings of terminal field development in controls differ drastically from the course of terminal field development proposed by Lasiter and coworkers (Lasiter, 1992; Lasiter et al., 1989). Earlier studies described an increase in terminal field size with increasing age, with the facial nerve (i.e., combined CT and GSP) terminal field becoming larger between P7 and P25 (Lasiter, 1992). According to previous findings, one might also expect the IX terminal field to be very small at P15 if it enters the NTS at P9–10 and increases in size until ~P45 (Lasiter, 1992). However, the current study shows that the IX terminal field is large at the youngest age examined (i.e., P15). These discrepancies may, in part, be due to the differences in techniques used by Lasiter and those used in our current study. Lasiter (1992) labeled the central stump of the facial nerve (i.e., both the CT and GSP nerves combined) in perfused preparations with Lucifer yellow and allowed the tracer to transport for 3–6 hours. In contrast, we used fluorescent tracers that were permitted to transport for 18–24 hours in live animals. In addition, brains were imaged using a scanning confocal laser microscope. Therefore, it is possible that more efficient tracer transport, longer survival times, and more sensitive imaging techniques account for the difference in the observed effects.

Proposed mechanisms for terminal field development in controls

Decreases in CT terminal field volume are coincident with the functional maturation of the taste system. That is, the largest decrease in volume occurs between P15 and P25; it is at approximately P25 when the CT nerve becomes maximally responsive to sodium salts (Ferrell et al., 1981; Hill and Almli, 1980; Yamada, 1980). The further decrease in CT terminal field volume at P35 corresponds with the period of sodium response maturation in the NTS (Hill et al., 1983). Unfortunately, similar comparisons between IX and GSP terminal fields with their functional maturation cannot be made because of the lack of corresponding functional data. It is important to note that maturation of the IX terminal field may not be as dependent on gustatory-evoked activity as hypothesized for the CT and GSP terminal fields, because the IX nerve has a

relatively larger tactile component (Frank, 1968). However, an argument for overall activity-dependent developmental pruning can be made for all three nerve terminal fields. That is, exuberant connections are made at young ages that are refined by increasing neural activity over the course of maturation of the system.

We find it especially interesting that the terminal fields of all three nerves share a significant volume of the gustatory NTS in controls at P15 (see Fig. 2). It is possible that these nerves project and expand within a circumscribed area rather indiscriminately during early development, relying predominantly on early target finding mechanisms. Each field may then rely on developmentally specific, taste-evoked activity ultimately to define the mature distinctiveness of each field. Thus, a more global activity-independent process(es) may set up the gustatory NTS early in development, followed by more activity-dependent mechanisms. This is consistent with the development of other sensory systems in which neural activity shapes terminal fields (Cummings and Brunjes, 1997; Deitch and Rubel, 1984; Hubel and Wiesel, 1970) via mechanisms related to pruning of axonal arbors (Kantor and Kolodkin, 2003) during postnatal development.

Proposed mechanisms for E3–E12 sodium-restricted development

In contrast to the decrease in terminal field volume that occurs in control rats, two of the three afferent terminal fields examined in E3–E12 sodium-restricted rats undergo significant enlargement at adulthood. Not only is this trend different from terminal field development in controls rats, it is also different from the lack of pruning of the CT nerve terminal field observed in rats that experience lifelong sodium restriction (Sollars et al., 2006). Namely, the terminal field of the CT changes little (or slightly decreases) during postnatal development in rats fed the sodium-restricted diet throughout development. The lack of the decrease in field volume is attributed to a corresponding lack of CT function (Sollars et al., 2006). Abnormally large terminal fields observed in E3–E12 restricted rats cannot be explained by a lack of appropriate sensory stimulation as with lifelong sodium restriction, because these rats receive a sodium-replete diet before the peripheral taste system is formed (Mistretta, 1972) and are maintained on a normal diet throughout postnatal development. Therefore, E3–E12 sodium-restricted rats receive normal sodium stimulation during development of the taste system. E3–E12 sodium-restricted rats display normal responsiveness of the CT nerve to sodium salts at adulthood (Mangold and Hill, 2007); thus, activity-dependent factors are probably not the main mechanism by which development in E3–E12 restricted rats is altered.

We believe that the altered development in early sodium-restricted rats probably is not due primarily to the reduction in maternal sodium for 9 days during pregnancy. Instead, we suggest that the effects result primarily from sodium repletion. It is likely that sodium repletion in these rats occurs during an early embryonic, critical period of neural development that leads to fundamental changes in the NTS and afferent terminal field morphology. Replenishment of sodium to the maternal diet at E12 occurs at a crucial time in gustatory system development, an age when geniculate ganglion cells are at their peak proliferation rate (E12) and during the differentiation of brainstem nuclei (E11–16; Altman and Bayer, 1982). From an earlier study, we know that ganglion cell numbers and NTS volumes are not affected (Mangold and Hill, 2007); however, cellular and/or molecular characteristics of NTS cells may be fundamentally different as a result of repletion. Such changes may relate to alterations in hormones and/or growth factors.

Maternal malnutrition results in the disruption of hormones and growth factors that can affect fetal brain development. Factors shown to be involved in altered brain development as a result of maternal malnutrition include glucocorticoids (Fleming et al., 2004; Owen et al., 2005), insulin, and insulin-like growth factors (IGFs; Barker, 1997; Lee et al., 1999). It is possible that any of these (or additional) factors play a role in the observed effects of prenatal sodium restriction. For example, maternal sodium restriction from E3 to E12 may lead to a rapid decrease in fetal IGF levels (Barker, 2001), which is important to brain development in general and to brainstem development in particular (Dentremont et al., 1999). It is possible that sodium repletion at E12 produces a surge in fetal IGF levels that is higher than normal during this important time for NTS development. Previous studies show similar trends for the relationship of malnutrition and brain IGF in other brain areas. For example, refeeding following food restriction leads to high levels of IGF-1 that persist into postnatal development and prolong the normal developmental time course (Chowen et al., 2002; Goya et al., 2002). A similar event may occur following sodium repletion at E12, potentially resulting in molecular/cellular alterations in the NTS that change the normal development of primary afferent terminal fields.

Implications and possible consequences

Regardless of the specific mechanisms involved in the shaping of mature terminal field organization in controls and in E3–E12 sodium-restricted rats, there are profound developmentally related changes for each group and equally profound differences between the groups. The age- and diet-dependent differences in terminal field organization may asffect the qualitative and quantitative coding of taste and tactile information in the gustatory NTS. For example, the degree of functional convergence of gustatory inputs onto NTS cells demonstrated in control animals (Travers et al., 1986; Vogt and Mistretta, 1990) may be altered significantly as a result of widely changing terminal fields during normal development and following an early environmental dietary manipulation. Changes in coding strategies may then affect taste-related behaviors and homeostatic processes as evidenced by changes in preference for sodium in rats sodium restricted during prenatal and early postnatal ages (Curtis et al., 2004; Thaw et al., 2000).

LITERATURE CITED

Altman J, Bayer S. 1982. Development of the cranial nerve ganglia and related nuclei in the rat. Adv Anat Embryol Cell Biol 74:1–90.

Barker DJ. 1997. Maternal nutrition, fetal nutrition, and disease in later life. Nutrition 13:807–813.

Barker DJ. 2001. The malnourished baby and infant. Br Med Bull 60:69–88.

Chowen JA, Goya L, Ramos S, Busiguina S, Garcia-Segura LM, Argente J, Pascual-Leone AM. 2002. Effects of early undernutrition on the brain insulin-like growth factor-I system. J Neuroendocrinol 14:163–169.

Cummings DM, Brunjes PC. 1997. The effects of variable periods of func-

tional deprivation on olfactory bulb development in rats. Exp Neurol 148:360–366.

Curtis KS, Krause EG, Wong DL, Contreras RJ. 2004. Gestational and early postnatal dietary NaCl levels affect NaCl intake, but not stimulated water intake, by adult rats. Am J Physiol Regul Integr Comp Physiol 286:R1043–R1050.

Deitch JS, Rubel EW. 1984. Afferent influences on brain stem auditory nuclei of the chicken: time course and specificity of dendritic atrophy following deafferentation. J Comp Neurol 229:66–79.

Dentremont KD, Ye P, D'Ercole AJ, O'Kusky JR. 1999. Increased insulin-like growth factor-I (IGF-I) expression during early postnatal development differentially increases neuron number and growth in medullary nuclei of the mouse. Brain Res Dev Brain Res 114:135–141.

Ferrell MF, Mistretta CM, Bradley RM. 1981. Development of chorda tympani taste responses in rat. J Comp Neurol 198:37–44.

Fleming TP, Kwong WY, Porter R, Ursell E, Fesenko I, Wilkins A, Miller DJ, Watkins AJ, Eckert JJ. 2004. The embryo and its future. Biol Reprod 71:1046–1054.

Frank ME. 1968. Single fiber responses in the glossopharyngeal nerve of the rat to chemical, thermal, and mechanical stimulation of the posterior tongue. PhD disssertation, Brown University, Providence, RI.

Goya L, Garcia-Segura LM, Ramos S, Pascual-Leone AM, Argente J, Martin MA, Chowen JA. 2002. Interaction between malnutrition and ovarian hormones on the systemic IGF-I axis. Eur J Endocrinol 147:417–424.

Halsell CB, Travers SP, Travers JB. 1996. Ascending and descending projections from the rostral nucleus of the solitary tract originate from separate neuronal populations. Neuroscience 72:185–197.

Hill DL. 1987. Susceptibility of the developing rat gustatory system to the physiological effects of dietary sodium deprivation. J Physiol 393:413–424.

Hill DL, Almli CR. 1980. Ontogeny of chorda tympani nerve responses to gustatory stimuli in the rat. Brain Res 197:27–38.

Hill DL, Przekop PR Jr. 1988. Influences of dietary sodium on functional taste receptor development: a sensitive period. Science 241:1826–1828.

Hill DL, Bradley RM, Mistretta CM. 1983. Development of taste responses in rat nucleus of solitary tract. J Neurophysiol 50:879–895.

Hubel DH, Wiesel TN. 1970. The period of susceptibility to the physiological effects of unilateral eye closure in kittens. J Physiol 206:419–436.

Kantor DB, Kolodkin AL. 2003. Curbing the excesses of youth: molecular insights into axonal pruning. Neuron 38:849–852.

King CT, Hill DL. 1991. Dietary sodium chloride deprivation throughout development selectively influences the terminal field organization of gustatory afferent fibers projecting to the rat nucleus of the solitary tract. J Comp Neurol 303:159–169.

Krimm RF, Hill DL. 1997. Early prenatal critical period for chorda tympani nerve terminal field development. J Comp Neurol 378:254–264.

Krimm RF, Hill DL. 1999. Early dietary sodium restriction disrupts the peripheral anatomical development of the gustatory system. J Neurobiol 39:218–226.

Lasiter PS. 1991. Effects of early postnatal receptor damage on dendritic development in gustatory recipient zones of the rostral nucleus of the solitary tract. Brain Res Dev Brain Res 61:197–206.

Lasiter PS. 1992. Postnatal development of gustatory recipient zones within the nucleus of the solitary tract. Brain Res Bull 28:667–677.

Lasiter PS. 1995. Effects of orochemical stimulation on postnatal development of gustatory recipient zones within the nucleus of the solitary tract. Brain Res Bull 38:1–9.

Lasiter PS, Kachele DL. 1990. Effects of early postnatal receptor damage on development of gustatory recipient zones within the nucleus of the solitary tract. Brain Res Dev Brain Res 55:57–71.

Lasiter PS, Wong DM, Kachele DL. 1989. Postnatal development of the rostral solitary nucleus in rat: dendritic morphology and mitochondrial enzyme activity. Brain Res Bull 22:313–321.

Lee KH, Calikoglu AS, Ye P, D'Ercole AJ. 1999. Insulin-like growth factor-I (IGF-I) ameliorates and IGF binding protein-1 (IGFBP-1) exacerbates the effects of undernutrition on brain growth during early postnatal life: studies in IGF-I and IGFBP-1 transgenic mice. Pediatr Res 45: 331–336.

Mangold JE, Hill DL. 2007. Extensive reorganization of primary afferent projections into the gustatory brainstem induced by feeding a sodium-restricted diet during development: less is more. J Neurosci 27:4650–4662.

May OL, Hill DL. 2006. Gustatory terminal field organization and developmental plasticity in the nucleus of the solitary tract revealed through triple-fluorescence labeling. J Comp Neurol 497:658–669.

Mistretta CM. 1972. Topographical and histological study of the developing rat tongue, palate and taste buds. In: Bosma JF, editor. Third symposium on oral sensation and perception. Springfield, IL: Thomas. p 163–187.

Ogawa H, Sato M, Yamashita S. 1968. Multiple sensitivity of chorda tympani fibres of the rat and hamster to gustatory and thermal stimuli. J Physiol 199:223–240.

Owen D, Andrews MH, Matthews SG. 2005. Maternal adversity, glucocorticoids and programming of neuroendocrine function and behaviour. Neurosci Biobehav Rev 29:209–226.

Pittman DW, Contreras R. 2002. Dietary NaCl influences the organization of chorda tympani neurons projecting to the nucleus of the solitary tract in rats. Chem Senses 27:333–341.

Shuler MG, Krimm RF, Hill DL. 2004. Neuron/target plasticity in the peripheral gustatory system. J Comp Neurol 472:183–192.

Smith JC, Miller IJ Jr, Krimm RF, Nejad MS, Beidler LM. 1988. A comparison of the effects of bilateral sections of the chorda tympani nerve and extirpation of the submaxillary and sublingual salivary glands on the eating and drinking patterns of the rat. Physiol Behav 44:435–444.

Sollars SI, Hill DL. 1998. Taste responses in the greater superficial petrosal nerve: substantial sodium salt and amiloride sensitivies demonstrated in two rat strains. Behav Neurosci 112:991–1000.

Sollars SI, Walker BR, Thaw AK, Hill DL. 2006. Age-related decrease of the chorda tympani nerve terminal field in the nucleus of the solitary tract is prevented by dietary sodium restriction during development. Neuroscience 137:1229–1236.

Thaw AK, Frankmann S, Hill DL. 2000. Behavioral taste responses of developmentally NaCl-restricted rats to various concentrations of NaCl. Behav Neurosci 114:437–441.

Travers SP, Pfaffmann C, Norgren R. 1986. Convergence of lingual and palatal gustatory neural activity in the nucleus of the solitary tract. Brain Res 365:305–320.

Vogt MB, Mistretta CM. 1990. Convergence in mammalian nucleus of solitary tract during development and functional differentiation of salt taste circuits. J Neurosci 10:3148–3157.

Whitehead MC. 1990. Subdivisions and neuron types of the nucleus of the solitary tract that project to the parabrachial nucleus in the hamster. J Comp Neurol 301:554–574.

Yamada T. 1980. Chorda tympani resonses to gustatory stimuli in developing rats. Jpn J Physiol 30:631–643.